2023 62nd IEEE Conference on Decision and Control (CDC)
December 13-15, 2023. Marina Bay Sands, Singapore

Boundary iterative learning control for repetitive spatio-temporal processes*

Maciej Patan[1], Kamil Klimkowicz[2], Krzysztof Patan[1] and Eric Rogers[3]

Abstract— **Iterative learning control for lumped processes is well established. Therefore, there is strong interest in developing designs that would produce similar flexibility for classes of distributed parameter systems. This paper develops a design for application to examples described by partial differential equations of convection-diffusion type in the multidimensional spatial domain, which have many applications, such as heat transfer problems. The system response is measured, and then the control is applied via specific boundary conditions using a sensor/actuator network, i.e., boundary control, as opposed to designs that require sensing and actuating application over the domain the dynamics are defined over. The convergence properties of the design are established in conjunction with rules for tuning its parameters for performance enhancement. Finally, the new design is applied to a laser heating problem in wafer staging, which requires boundary control.**

I. INTRODUCTION

Iterative learning control (ILC) originated in the mid-1980s [1]. It applies to systems that repeatedly complete the same finite-duration task. The 'pick and place task that arises in many industrial applications is a particular example in robotics. The mode of operation in pick and place is to transfer a sequence of payloads from a specified location over a finite time and place them, under synchronization, on a moving conveyor. Moreover, the sequence of operations by the robot are: Collect a payload from the specified location. Transfer it over a finite duration. Place the payload on the conveyor. Return to the starting location, collect the next payload, and so on. The term trial is used to distinguish which particular payload is under consideration, and its duration from pick to place is termed the trial length (other terms are used in some of the literature). Once a trial is complete, all information generated is available to design the control to be applied on the next trial.

Suppose that a reference trajectory is specified for an application. Then on any trial, the error is the difference between this trajectory and the output on each trial. Each trial error forms the corresponding entry in the error sequence over all trials. The design problem is to design control action such that this error sequence converges with an increasing trial number and regulates the response along the trials.

In ILC, the input (a signal) is adjusted as opposed to a controller (a system) in other control system designs. Possible sources for the early literature are the survey papers [2], [3]. For more recent theoretical developments and applications, including outside engineering, see, e.g., [4].

The critical feature of a system to which ILC can be applied is the repetition of the same finite duration task, with either i) resetting to a fixed location after each is complete or ii) the end of one trial and the start of the next are not co-incidental. Hence ILC can also be applied to some batch processing operations, e.g., in the process industries. This paper focuses on systems described by partial differential (or distributed parameter systems (DPSs) operating in batch processing mode.

One approach to DPS analysis and control is to work with the governing partial differential equation, e.g., the heat or wave equations, and one starting point for the literature (up to the time of publication) is the research text [5]. Other problem areas must, however, start with a numerical solution of the governing equations due, e.g., to the complexity of the dynamics, the boundary conditions, and the sensing and actuating choices available. Such problems arise across a range of application areas, see, e.g., [6]–[9].

A general application area for ILC in DPS is operations where a sequence of workpieces are processed over the same time interval, i.e., one workpiece is replaced by another, introducing a time between the completing the processing of one workpiece and starting to process the next. Previous results on ILC for DPS include [10], but the results are limited to one spatial dimension.

Recent work on ILC for DPS using distributed sensing and actuation includes [11], [12]. The results in [11] relate to application in flexible materials, while the paper [12] and extends the results in [11] to systems with a multi-dimensional spatial domain modeled by a parabolic partial differential equation with convection and diffusion components. In addition, a decentralized control update strategy has been developed. These results can only be used to design control actions that can be applied across the domain of the example considered. In my cases, however, control action can only be applied at the domain's boundary.

This paper extends the previous results to allow boundary control and the novel contributions are: (1) the development of a boundary PD-type ILC law for the class of parabolic distributed parameter systems in multidimensional spatial domain described by partial differential equations of diffusion-convection with steady velocity field type, (2) a convergence analysis to provide sufficient conditions, (3) development of a procedure to tune the learning gain matrices based on the convergence conditions, and (4) application to heating of a

*This work was supported by the National Science Center in Poland, grant No. 2020/37/B/ST7/03280

[1]Institute of Control and Computation Engineering, University of Zielona Góra, Poland, {m.patan,k.patan}@issi.uz.zgora.pl

[2]Institute of Control, Electronic and Electric Engineering, University of Zielona Góra, Poland, k.klimkowicz @iee.uz.zgora.pl

[3]Eric Rogers is with the Department of Electronics and Computer Science, University of Southampton, UK, etar@ecs.soton.ac.uk

rotating silicon wafer to demonstrate the application of the design.

II. SYSTEM DESCRIPTION

The subject area is spatio-temporal processes represented by the convection-diffusion partial differential equation, where the time interval $T = [0, t_f]$ is finite and $\Omega \subset \mathbb{R}^3$ is a bounded spatial domain with a boundary $\partial\Omega$. Moreover, the scalar state of this process at the spatial point $x \in \bar{\Omega} \subset \mathbb{R}^3$ at time $t \in \bar{T}$ is denoted as $y(x,t)$. The mathematical model is

$$\begin{aligned}\frac{\partial y(x,t)}{\partial t} &+ \nabla \cdot \big(\boldsymbol{v}(x) y(x,t)\big) \\ &= \nabla \cdot \big(\kappa \nabla y(x,t)\big) + f(x,t), \quad (x,t) \in \Omega \times T\end{aligned} \tag{1}$$

where κ denotes a turbulent diffusion coefficient, $\boldsymbol{v}(x)$ represents a steady velocity field vector, and $f(x,t)$ denotes some known function representing a source. The system has initial and boundary conditions (of the general Robin type):

$$\begin{cases} y(x,0) = y_0, & x \in \Omega, \\ \boldsymbol{n} \cdot \big(\boldsymbol{v}(x) y(x,t) - \kappa \nabla y(x,t)\big) = g(x,t), & (x,t) \in \partial\Omega \times T, \end{cases} \tag{2}$$

where $\boldsymbol{n}$ is the outward normal vector to the boundary $\partial\Omega$. Physically $g(x,t)$ represents the total flux (i.e., the sum of the convective and diffusion fluxes) at the boundary. Simultaneously, it represents an external control action on the boundary due to actuation using m devices. For practical control design, implementation is by a form of control-affine approximation, i.e.,

$$g(x,t) = \sum_{i=1}^{m} q_i(x) u_i(t) \tag{3}$$

and $u_i(t)$ is the control signal of the i-th actuator. Also, $q_i(x)$ denotes a spatial distribution of actuation, which is a non-negative integrable function satisfying the normalization condition, i.e.,

$$\int_{\partial\Omega} q_i(x) \mathrm{d}s = 1, \tag{4}$$

The above abstract definition of the actuation field includes a wide variety of practical situations, from pointwise local actuation, i.e., q_i is a Dirac's delta distribution, to fully distributed control over the entire boundary. Further, it is assumed that the system output is observed continuously over an interval T by the array of $n \leq m$ sensors in the consecutive trials of the process. The measurements can be mathematically described as

$$z_k^j(t) = \int_\Omega p_j(x) y_k(x,t) \mathrm{d}x, \ t \in T, \ j = 1, \ldots, n \tag{5}$$

where k is the trial number, $\boldsymbol{u}_k(t) = [u_{k1}(t), \ldots, u_{km}(t)]^\mathsf{T}$ is the control input vector at k-th trial and $y_k(x,t) = y(x,t;\boldsymbol{u}_k(t))$. Observations taken, e.g., by the j-th individual sensor is characterized by a spatial distribution $p_j(x)$ defined on the domain Ω with $\int_\Omega p_j(x) \mathrm{d}x = 1$.

The probability density p_j can be interpreted as the proportion of observational effort dedicated to a particular spatial location (e.g., measurement replications), measurement procedure (e.g., integration or averaging by measurement transducers), or accuracy at different spatial positions. Again, such an abstract formulation of observations has commonality with modern optimum experimental design theory, e.g., [11], [13]. Moreover, it covers numerous measurement scenarios, from pointwise local measurements (e.g., a Dirac delta distribution) to fully distributed global observations (e.g., uniform distribution over the entire area). Also, it allows the implementation of both the in-domain measurements (joint probability distribution over Ω) and boundary observations (boundary probability distribution over $\partial\Omega$).

III. ITERATIVE LEARNING CONTROL

A. Control law

The control objective is to modify form the input signal vector $\boldsymbol{u}_k(t)$ such the measurement output vector $\boldsymbol{z}_k(t) = [z_k^1(t), \ldots, z_k^n(t)]^\mathsf{T}$ follows some differentiable reference trajectory $\boldsymbol{z}_{\text{ref}}(t)$ with arbitrary accuracy. In particular, the objective is to sequentially improve performance from trial to trial such that the tracking error norm:

$$\|\boldsymbol{e}_k(t)\| = \|\boldsymbol{z}_k(t) - \boldsymbol{z}_{\text{ref}}(t)\| \tag{6}$$

converges as $k \to \infty$ to, ideally, zero or some specified tolerance. This paper uses a feedforward ILC scheme, where measurement data gathered from the previous trial is used to update the control input for the subsequent trial based on the tracking error [1], [11], [14]. In particular, the control law has the structure

$$\boldsymbol{u}_{k+1}(t) = \boldsymbol{u}_k(t) + \boldsymbol{\Lambda}_k \dot{\boldsymbol{e}}_k(t) + \boldsymbol{\Upsilon}_k \boldsymbol{e}_k(t) \tag{7}$$

where $\boldsymbol{\Lambda}_k, \boldsymbol{\Upsilon}_k \in R^{m \times n}$ are learning coefficients matrices. Also

- setting $\boldsymbol{\Upsilon}_k = 0$ results in the so-called D-type law,
- setting $\boldsymbol{\Lambda}_k = 0$ results in the so-called P-type law.

B. Convergence Analysis

The following assumptions underpin the analysis in this section.

A1. Let $\boldsymbol{z}_{\text{ref}}(t)$ be a vector of reference trajectories preselected over a finite time interval T. Moreover, it is assumed that $\boldsymbol{z}_{\text{ref}}(t)$ is realizable, i.e., there exists a unique $\boldsymbol{u}_{\text{ref}}(t) = [u_{\text{ref},1}, \ldots, u_{\text{ref},m}]^\mathsf{T}$ with the initial state $y_{\text{ref}}(x,0) = 0$ such that

$$\begin{aligned}\frac{\partial y_{\text{ref}}(x,t)}{\partial t} &+ \nabla \cdot \big(\boldsymbol{v}(x) y_{\text{ref}}(x,t)\big) \\ &= \nabla \cdot \big(\kappa \nabla y_{\text{ref}}(x,t)\big) + f(x),\end{aligned} \tag{8}$$

$$\boldsymbol{n} \cdot (\boldsymbol{v}(x) y_{\text{ref}} - \kappa \nabla y_{\text{ref}}) = \boldsymbol{q}(x)^\mathsf{T} \boldsymbol{u}_{\text{ref}}(t) \tag{9}$$

where $\boldsymbol{q}(x) = [q_1(x), \ldots, q_m(x)]^\mathsf{T}$ and

$$\boldsymbol{z}_{\text{ref}}^j(t) = \int_\Omega p_j(x) y_{\text{ref}}(x,t) \mathrm{d}x, \ t \in T, \ j = 1, \ldots, n. \tag{10}$$

A2. It is assumed that the same initial conditions hold for all trials, i.e.

$$\forall k, \ \ y_k(x,0) = y_{\text{ref}}(x,0) = 0. \tag{11}$$

The assumptions (A1)–(A2) are typical in iterative learning control. Their interpretation is clear as they are related to the reproducibility of the same experimental conditions for each trial. In the context of the considered system, the following assumption is also required.

A3. The measurement distributions, i.e., the p_j, belong to the class of piecewise constant functions, i.e., assuming the partition of the domain Ω into a finite number L_j of disjoint subdomains Ω_ℓ such that $\Omega = \cup_{\ell=1}^{L_j}\Omega_\ell$, then $p_j(x) = \sum_{\ell=1}^{L_j} p_j^\ell(x)$, where

$$p_j^\ell(x) = \begin{cases} p_j^\ell > 0 & \text{for } x \in \Omega_\ell \\ 0 & \text{otherwise} \end{cases}. \tag{12}$$

This last assumption introduces some basic approximation (with assumed a priori accuracy) for measurement distribution with a possible low level of complexity which leads to a dramatic simplification of the control design. The idea is similar to local basis functions in the finite element method.

The following theorem establishes convergence properties for the PD-type controller.

Theorem 1: Suppose that assumptions (A1)–(A3) hold. Then, under the ILC law (7) applied to the system (1)–(2), the error (6) converges uniformly if the following conditions hold

$$\|\boldsymbol{I} - \boldsymbol{R}\boldsymbol{\Lambda}_k\| < 1 \quad \text{and} \quad \|\boldsymbol{R}\boldsymbol{\Upsilon}_k\| > 0 \tag{13}$$

where $\boldsymbol{R} \in \mathbb{R}^{n\times m}$ with $R_{ij} = \int_{\partial\Omega} p_j(x)q_i(x)\mathrm{d}s$.

Proof: Subtracting the system state equations (1) at two consecutive trials gives

$$\begin{aligned}\frac{\partial}{\partial t}(y_{k+1}(x,t) - y_k(x,t)) + \nabla\cdot\big(\boldsymbol{v}(x)(y_{k+1}(x,t) - y_k(x,t)\big) \\ = \nabla\cdot\kappa\nabla(y_{k+1}(x,t) - y_k(x,t))\end{aligned} \tag{14}$$

Multiplying (14) by the j-th sensor spatial distribution p_j and introducing $\tilde{y}_k(x,t) = y_{k+1}(x,t) - y_k(x,t)$ results in

$$\begin{aligned}p_j(x)\frac{\partial}{\partial t}\tilde{y}_k(x,t) + p_j(x)\nabla\cdot\boldsymbol{v}(x)\tilde{y}_k(x,t) \\ = p_j(x)\nabla\cdot\kappa\nabla\tilde{y}_k(x,t).\end{aligned} \tag{15}$$

Integrating this last equation on Ω and applying the Leibniz integral rule for the first integral on the left-hand side gives

$$\begin{aligned}\frac{\mathrm{d}}{\mathrm{d}t}\int_\Omega p_j(x)\tilde{y}_k(x,t)\mathrm{d}x + \int_\Omega p_j(x)\nabla\cdot\boldsymbol{v}(x)\tilde{y}_k(x,t)\mathrm{d}x \\ = \int_\Omega p_j(x)\nabla\cdot\kappa\nabla\tilde{y}_k(x,t)\mathrm{d}x\end{aligned} \tag{16}$$

Applying the Gauss (or Ostrogradsky) theorem to the second integral on the left-hand side of (16) and applying the Green's formula to rewrite the integral on the right-hand side of (16) gives

$$\begin{aligned}&\frac{\mathrm{d}}{\mathrm{d}t}\int_\Omega p_j(x)\tilde{y}_k(x,t)\mathrm{d}x + \int_{\partial\Omega} p_j(x)\boldsymbol{n}\cdot\boldsymbol{v}(x)\tilde{y}_k(x,t)\mathrm{d}s \\ &\quad - \int_\Omega \nabla p_j(x)\cdot\boldsymbol{v}(x)\tilde{y}_k(x,t)\mathrm{d}x \\ &\quad = \int_{\partial\Omega} p_j(x)\boldsymbol{n}\cdot\kappa\nabla\tilde{y}_k(x,t)\mathrm{d}s \\ &\quad - \int_\Omega \nabla p_j(x)\cdot\kappa\nabla\tilde{y}_k(x,t)\mathrm{d}x\end{aligned} \tag{17}$$

where $\mathrm{d}s$ represents a boundary element of Ω. Under assumption (A3) for the class of piecewise constant functions, $\nabla p_j(x) = 0$ almost everywhere. Note that the discontinuities of $p_j(x)$'s are located in the subset of Ω with measure zero. Hence the last integrals can be eliminated over domain Ω on both sides of (17), respectively. Hence after some rearrangement

$$\begin{aligned}&\frac{\mathrm{d}}{\mathrm{d}t}\int_\Omega p_j(x)\tilde{y}_k(x,t)\mathrm{d}x \\ &= -\int_{\partial\Omega} p_j(x)\boldsymbol{n}\cdot\big(\boldsymbol{v}(x)\tilde{y}_k(x,t) - \kappa\nabla\tilde{y}_k(x,t)\big)\mathrm{d}s\end{aligned} \tag{18}$$

Using the boundary condition (2) combined with the control update (7) the last set of equations (for $j = 1,\ldots,n$) can be written in the form:

$$\begin{aligned}&\frac{\mathrm{d}}{\mathrm{d}t}\int_\Omega \boldsymbol{p}(x)\tilde{y}_k(x,t)\mathrm{d}x \\ &\quad = -\int_{\partial\Omega}\boldsymbol{p}(x)\boldsymbol{q}^\mathsf{T}(x)\big(\boldsymbol{\Lambda}_k\dot{\boldsymbol{e}}_k(t) + \boldsymbol{\Upsilon}_k\boldsymbol{e}_k(t)\big)\mathrm{d}s \\ &\quad = -\boldsymbol{R}\boldsymbol{\Lambda}_k\dot{\boldsymbol{e}}_k(t) - \boldsymbol{R}\boldsymbol{\Upsilon}_k\boldsymbol{e}_k(t),\end{aligned} \tag{19}$$

where $\boldsymbol{p}(x) = [p_1(x),\ldots,p_n(x)]^\mathsf{T}$.

From the definition of the tracking error, it follows that

$$\begin{aligned}\dot{\boldsymbol{e}}_{k+1}(t) &= \dot{\boldsymbol{z}}_{k+1}(t) - \dot{\boldsymbol{z}}_{\mathrm{ref}}(t) \\ &= \dot{\boldsymbol{e}}_k(t) + (\dot{\boldsymbol{z}}_{k+1}(t) - \dot{\boldsymbol{z}}_k(t)) \\ &= \dot{\boldsymbol{e}}_k(t) + \frac{\mathrm{d}}{\mathrm{d}t}\int_\Omega \boldsymbol{p}(x)\tilde{y}_k(x,t)\mathrm{d}x \\ &= \dot{\boldsymbol{e}}_k(t) - \boldsymbol{R}\boldsymbol{\Lambda}_k\dot{\boldsymbol{e}}_k(t) - \boldsymbol{R}\boldsymbol{\Upsilon}_k\boldsymbol{e}_k(t).\end{aligned} \tag{20}$$

Integration of (20) with respect to time with the initial condition satisfying (A2) gives

$$\boldsymbol{e}_{k+1}(t) = \big(\boldsymbol{I} - \boldsymbol{R}\boldsymbol{\Lambda}_k\big)\boldsymbol{e}_k(t) - \boldsymbol{R}\boldsymbol{\Upsilon}_k\int_0^t \boldsymbol{e}_k(\tau)\mathrm{d}\tau, \tag{21}$$

where $\boldsymbol{I}$ is the compatibly dimensioned identity matrix.

Taking the norm on both sides of (21) gives

$$\begin{aligned}\|\boldsymbol{e}_{k+1}(t)\| &= \|\big(\boldsymbol{I} - \boldsymbol{R}\boldsymbol{\Lambda}_k\big)\boldsymbol{e}_k(t) - \boldsymbol{R}\boldsymbol{\Upsilon}_k\int_0^t \boldsymbol{e}_k(\tau)\mathrm{d}\tau\| \\ &\le \|\big(\boldsymbol{I} - \boldsymbol{R}\boldsymbol{\Lambda}_k\|\|\boldsymbol{e}_k(t)\| + \|\boldsymbol{R}\boldsymbol{\Upsilon}_k\|\Big\|\int_0^t \boldsymbol{e}_k(\tau)\mathrm{d}\tau\Big\|.\end{aligned} \tag{22}$$

By definition, the error $\boldsymbol{e}_k(t)$ is bounded on the finite time interval T, and the norm of the integral in (22) is also bounded, and satisfies $\big\|\int_0^t \boldsymbol{e}_k(\tau)\mathrm{d}\tau\big\| \le \epsilon_p$ for some positive

constant ϵ_p. Introducing $\gamma_d = \sup_k \|\boldsymbol{I} - \boldsymbol{R}\boldsymbol{\Lambda}_k\|$ and $\gamma_p = \sup_k \|\boldsymbol{R}\boldsymbol{\Upsilon}_k\|$ from (22) gives

$$\|\boldsymbol{e}_{k+1}(t)\| - \gamma_d \|\boldsymbol{e}_k(t)\| \leq \gamma_p \epsilon_p. \tag{23}$$

Also, see [15], (23) is satisfied if $\gamma_1 < 1$ and $\gamma_2 > 0$. Hence

$$\lim_{k\to\infty} \|\boldsymbol{e}_k(t)\| \leq \frac{\gamma_p \epsilon_p}{1-\gamma_d}. \tag{24}$$

Since the q_i's and p_j's are nonnegative distributions, therefore by definition, R_ij's takes nonnegative values for any i and j. Hence, there exists $\boldsymbol{\Lambda}_k$ such that

$$\|\boldsymbol{I} - \boldsymbol{R}\boldsymbol{\Lambda}_k\| < 1. \tag{25}$$

Let $\boldsymbol{e}(t)$ denote the pointwise limit of the error $\boldsymbol{e}_k(t)$ with $k \to \infty$. Then, in the case of $\boldsymbol{\Upsilon}_k = \boldsymbol{0}$, the D-type control law, it follows immediately from (24) that

$$\lim_{k\to\infty} \|\boldsymbol{e}_k(t)\| = 0,$$

i.e., $\boldsymbol{e}(t) = \boldsymbol{0}$. Otherwise, from (20) it is concluded that $\boldsymbol{e}(t)$ is the solution to the following Cauchy initial value problem

$$\boldsymbol{R}\boldsymbol{\Lambda}\dot{\boldsymbol{e}}(t) = -\boldsymbol{R}\boldsymbol{\Upsilon}\boldsymbol{e}(t), \quad \boldsymbol{e}(0) = \boldsymbol{0}, \tag{26}$$

for $\boldsymbol{\Lambda}$ and $\boldsymbol{\Upsilon}$ satisfying (13). The zero initial condition is a direct consequence of assumption (A2). It can be easily shown that in the case of full rank matrices $\boldsymbol{R}\boldsymbol{\Lambda}$ and $\boldsymbol{R}\boldsymbol{\Upsilon}$ the particular solution of the system of equations (26) is $\boldsymbol{e}(t) = \boldsymbol{0}$. Hence the error sequence uniformly converges to zero, and the proof is complete.

$$\lim_{k\to\infty} \boldsymbol{e}_k(t) = 0.$$

■

Theorem 1 is a sufficient condition for the convergence of the PD ILC law and is an alternative to the in-domain control strategies developed in [11], [12] for the hyperbolic and parabolic systems class.

Remark 1: Theorem 1, allows decoupling the control update, leading to an even easier implementation of the ILC design. In particular, attention can be restricted to diagonal learning matrices (but at the cost of some performance reduction). In fact, considering the ILC law (7) with $m = n$, $\boldsymbol{\Upsilon}_k = \boldsymbol{0}$ and diagonal learning matrix $\boldsymbol{\Lambda}_k$ with $\lambda_k^j, j = 1, \ldots, n$ denoting its diagonal elements, (21) can be written as

$$e_{k+1}^i(t) = e_k^i(t) - \sum_{j=1}^{n} R_{ij}\lambda_k^j e_k(t), \quad i = 1, \ldots, n. \tag{27}$$

Moreover, the i-th component of tracking error on trial $k+1$ is a linear combination of error components from trial k. Hence a solution to the following problem is required:

Problem 1: Find $\lambda_k^j, j = 1, \ldots, n$, subject to

$$-1 < 1 - \sum_{j=1}^{n} R_{ij}\lambda_k^j < 1, \quad i = 1, \ldots, n. \tag{28}$$

This problem is a relatively simple linear feasible solution problem, and the solution inside the polyhedral defined by (28) guarantees convergence of control update. The solution exists if the matrix R has linearly independent rows, i.e., has full rank.

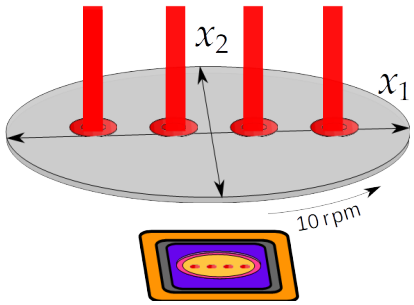

Fig. 1. Silicon disk heating using four laser beams with infrared vision camera monitoring lower surface

Once the D-type control update is determined, the matrix Υ_k can be used to speed up convergence rate. Finally, the adopted control design in each trial is a two step procedure: first solve the Problem 1 and determine the coefficients of Λ_k matrix, then heuristically tune the Υ_k matrix as to increase the convergence rate.

IV. Case Study

The case study arises from the problem of heating silicon disks one after another. Four laser beams, arranged evenly along the disk diameter, apply heat to a very thin rotating disk. The disc diameter is $d = 0.054$ m, and its thickness is 0.0003 m. In particular, the heating of each disk lasts 60 seconds, after which the disk is replaced with the next one, and the process is repeated again and again. This application is one where ILC can be applied (a finite duration task is completed, and there is a stoppage time before the task is repeated); hence, information from one completion is available to update the control law for the next). The disk moves in one direction at a constant rotational speed of 10 rpm. Each laser beam is applied to the disk over a circle with radius $r = 0.002$ m around its focal point, and the maximum power is 15 W (see Fig. 1).

The action of the i-th laser beam on the upper surface of a silicon disk is a combination of the beam intensity $u_i(t)$ and the spatial distribution of the beam $q_i(x)$, and is represented by the Gaussian distribution:

$$q_i(x) = \sqrt{\frac{2}{\pi r^2}} \exp\Big(-2\frac{(x_1 - d(1-0.2i))^2 + x_2^2}{r^2}\Big). \tag{29}$$

where x_1 and x_2 are the coordinates of the spatial point x. It is assumed that the laser operates at a wavelength at which the wafer is opaque, and in this manner, all of the laser heat is deposited at the surface. In the case considered, the disk emissivity ϵ is also taken into account, which has a value of 0.8. Additionally, it is assumed that the constant ambient temperature θ_0 is set to 293.15 K.

To complete the problem specified in Section II, the time interval is taken as $T = (0.60]$ and the spatial domain $\Omega = \{(x_1, x_2, x_3) : x_1^2 + x_2^2 \leq 0.0254^2, x_3 \in [0.3 \cdot 10^{-4}]\} \subset \mathbb{R}^3$. For this application, the PDE (1) is rewritten as

$$\rho C_p \frac{\partial \bar{\theta}(x,t)}{\partial t} + \rho C_p v(x) \cdot \nabla \bar{\theta}(x,t) - \nabla \cdot \kappa \nabla \bar{\theta}(x,t) = 0, \tag{30}$$

where ρ is the mass density per unit area, C_p stands for the thermal capacity of silicon, κ represents the thermal conductivity, $v(x) = \frac{\pi}{3} \cdot [-x_2, x_1]^{\mathsf{T}}$ is the speed field. Due to the zero initial conditions, in (30), the difference between the disk and ambient temperature $\bar{\theta}$ is used.

Heat losses are treated as radiation from the upper disk surface to the surrounding environment (where this assumption requires perfect disk insulation but is valid for initial control design verification studies). The boundary and initial conditions are of the form of (2) with

$$g(x,t) = \begin{cases} \epsilon \sum_{i=1}^{4} q_i(x) u_i(t), & x \in \Gamma_1, \ t \in T, \\ 0, & x \in \Gamma_2, \ t \in T, \end{cases} \tag{31}$$
$$\bar{\theta}(x,0) = 0, \quad x \in \Omega,$$

where the Γ_1 is the upper surface of wafer, and $\partial\Omega = \Gamma_1 \cup \Gamma_2$. The heating profile does introduce significant temperature variations since the linear velocity outside the wafer is greater. Thus the laser heat deposits over a larger area in the same time duration. The disk's temperature is acquired from the thermal imaging camera placed underside of the disk. The disk is divided into symmetric quadrants designated by the x_1 and x_2 axes (see Fig. 1), and for each quadrant the average temperature is derived. The objective of the control is to obtain an average temperature course for each quadrant defined by the following temperature profile:

$$z_{\text{ref}}(t) = 50 \cdot \sin(0.0083\pi t), \quad t \in [0, 60]. \tag{32}$$

Also, the results given in the remainder of this paper were obtained using a COMSOL MULTIPHISICS 5.4 and MATLAB 2018b software computer with the Intel Core i7 1.99 GHz processor and 16 GB of RAM. The solver used a spatial grid with 780 nodes and 1044 triangular prisms.

The rest of the paper uses a digital approximation (constructed as above) to investigate critical aspects of control performance for D and PD-type laws and their relative performance. The first area investigated is the effects of different choices of the learning gain matrix on performance. Three forms of learning gain are examined, namely full, diagonal, and tridiagonal control law matrices. Convergence results for the tracking performance are expressed in the form of the mean squared tracking error (MSE) computed along the trial, and the results are given in Figs. 2, 3 and 4. In these figures, the results for the D-type controller are in solid red color and those for the PD controller in the blue-dashed color.

Analyzing the results in Figs. 2, 3 and 4, it is immediate in each case that the PD controller converges faster than the D-type. However, in two cases, for the full and tridiagonal learning matrices, the PD-type controller exhibits worse convergence than the D-type controller over the initial trials (see the upper-left zoomed windows in Figs. 2 and 4). An explanation of this phenomenon could be the application of learning gain matrices in the form of a full or tridiagonal matrix, which makes it possible to consider interactions between actuators (laser beams).

In contrast, in the case of the diagonal matrix, no account of the interactions between the actuators is enforced. In such a case, the proportional term of the controller is more sensitive to the form of the gain matrix than the derivative term. These results demonstrate that the PD controller with the full learning gain matrix is the best of the three options. Summarizing this part of experiments we can conclude that introducing the proportional term to the controller makes it possible to achieve much faster convergence of the error trace.

The next part of the experiments investigates the temperature evolution of the disk surface along successive trials.

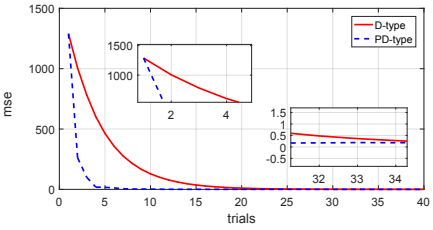

Fig. 3. Convergence results for a diagonal learning matrix

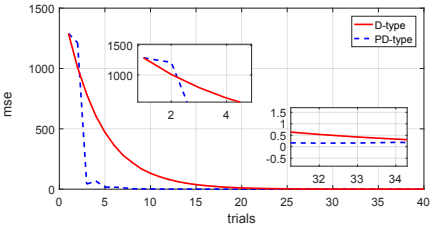

Fig. 4. Convergence results for a tridiagonal learning matrix

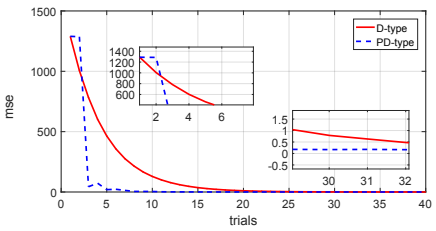

Fig. 2. Convergence results for a full learning matrix

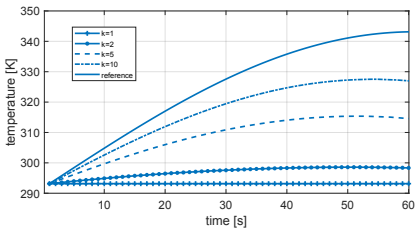

Fig. 5. Evolution of temperature for the D controller

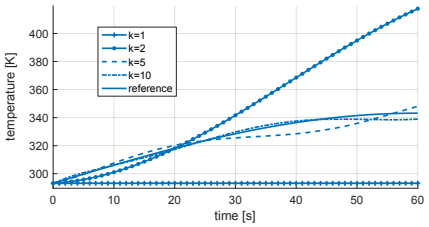

Fig. 6. Evolution of temperature for the PD controller

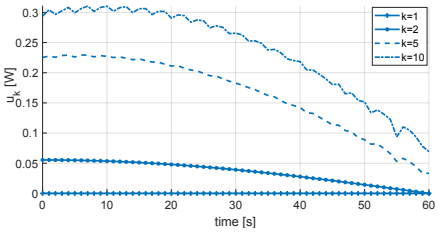

Fig. 7. Control signal evolution of the 1st laser beam with the D-type controller

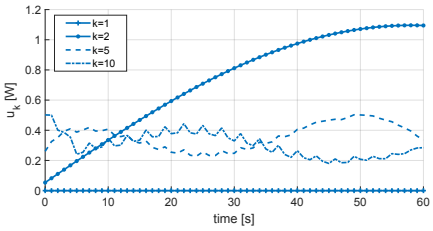

Fig. 8. Control signal evolution of the 1st laser beam with PD-type controller

For the D-type controller, the average temperature over the disk for selected trials is shown in Fig. 5. From trial to trial, the temperature curve leads to the required reference profile (marked with the solid line), but very slowly. In this case, the temperature curve is smooth and slowly changing. In turn, the temperature evolution achieved for PD-type ILC is shown in Fig. 6, where, in this case, a rapid change in the temperature profile occurs, especially for the initial trials. After that, the temperature profile is driven near the reference. The temperature changes are smaller for future trials, but contrary to the D-type, the temperature variability is quite significant.

The last aspect investigated is the control signal required, where the system consists of four actuators, and hence four control signals. However, for the clarity of presentation, the control signal of one laser only is considered. (For the other lasers, the results are quite similar). The evolution of the control signal for the first laser with the D-type law is shown in Fig. 7. Similar to the temperature, the control signal converge relatively slowly. The oscillations observed for the later trials are numerical and are closely related to the computation of the first derivative of the tracking error. Fig. 8 gives the control signal evolution of the first laser for the PD learning controller. In this case, faster convergence to the required control sequence is observed. As a particular case, For the 10-th trial, the control signal fluctuates around $u_{10} \approx 0.3$. Finally, note that the control objective is achieved using a relatively small power for the first laser of less than 0.5 W.

V. Conclusions and Future Research

The paper has considered iterative learning control applied to a general class of parabolic distributed parameter systems with control applied via the boundary conditions. Two laws have been investigated, D- and PD-type, and their convergence properties were established. These properties are straightforward to apply and can be constructively used to tune the learning gain matrices.

Future research will address the important issue of generalization of the approach to address measurement and model prediction errors, together with optimization of sensor/actuator locations for improving control quality.

References

[1] S. Arimoto, S. Kawamura, and F. Miyazaki, "Bettering operation of robots by learning," *Journal of Robotic systems*, vol. 1, no. 2, pp. 123–140, 1984.

[2] D. A. Bristow, M. Tharayil, and A. G. Alleyne, "A survey of iterative learning control: a learning-based method for high-performance tracking control," *IEEE Control Systems Magazine*, vol. 26, no. 3, pp. 96–114, 2006.

[3] H.-S. Ahn, Y. Chen, and K. L. Moore, "Iterative learning control: brief survey and categorization," *IEEE Transactions on Systems Man and Cybernetics Part C Applications and Reviews*, vol. 37, no. 6, p. 1099, 2007.

[4] E. Rogers, B. Chu, C. T. Freeman, and P. L. Lewin, *Iterative Learning Control Algorithms and Experimental Benchmarking*. Chichester: Wiley, 2023.

[5] R. F. Curtain and H. Zwart, *An introduction to infinite-dimensional linear systems theory*. Springer Science & Business Media, 2012, vol. 21.

[6] W. F. Ames, *Numerical methods for partial differential equations*. Academic press, 2014.

[7] D. G. Cacuci, I. M. Navon, and M. Ionescu-Bujor, *Computational Methods for Data Evaluation and Assimilation*. Boca Raton, FL: CRC, 2014.

[8] N.-Z. Sun and A. Sun, *Model Calibration and Parameter Estimation For Environmental and Water Resource Systems*. New York: Springer, 2015.

[9] K. Patan and M. Patan, "Fault-tolerant design of non-linear iterative learning control using neural networks," *Engineering Applications of Artificial Intelligence*, vol. 124, no. 106501, pp. 1–13, 2023.

[10] X.-S. Dai, X.-Y. Zhou, S.-P. Tian, and H.-T. Ye, "Iterative learning control for mimo singular distributed parameter systems," *IEEE Access*, vol. 5, pp. 24 094–24 104, 2017.

[11] M. Patan, K. Klimkowicz, R. Maniarski, K. Patan, and E. Rogers, "Iterative learning control of the displacements of a cantilever beam," in *58th IEEE Conference on Decision and Control, CDC 2019, Nice, France*, 5593–5598, p. 2019.

[12] M. Patan, K. Klimkowicz, and K. Patan, "Iterative learning control for distributed parameter systems using sensor-actuator network," in *16th International Conference on Control Automation Robotics and Vision, ICARCV 2020*, 1200–1205, p. 2020.

[13] M. Patan, *Optimal sensor networks scheduling in identification of distributed parameter systems*. Springer Science & Business Media, 2012, vol. 425.

[14] M. Patan, K. Patan, K. Gałkowski, and E. Rogers, "Iterative learning control of repetitive transverse loads in elastic materials," in *57th IEEE Conference on Decision and Control, CDC 2018, Miami, FL, USA, December 17-19, 2018*, 2018, pp. 5270–5275. [Online]. Available: https://doi.org/10.1109/CDC.2018.8619699

[15] C.-J. Chien, "A discrete iterative learning control for a class of nonlinear time-varying systems," *IEEE Transactions on Automatic Control*, vol. 43, no. 5, pp. 748–752, 1998.